

**Greenhouse gases emissions from riparian wetlands: An example from the Inner  
Mongolia grassland region in China**

**Xinyu Liu<sup>1,2</sup>, Xixi Lu<sup>1,3</sup>, Ruihong Yu<sup>1,2</sup>, Heyang Sun<sup>1</sup>, Hao Xue<sup>1</sup>, Zhen Qi<sup>1</sup>,  
Zhengxu Cao<sup>1</sup>, Zhuangzhuang Zhang<sup>1</sup>, Tingxi Liu<sup>4</sup>**

<sup>1</sup> Inner Mongolia Key Laboratory of River and Lake Ecology, School of Ecology and Environment,  
Inner Mongolia University, Hohhot 010021, China;

<sup>2</sup> Key Laboratory of Mongolian Plateau Ecology and Resource Utilization, Ministry of Education,  
Hohhot 010021, China;

<sup>3</sup> Department of Geography, National University of Singapore, 117570, Singapore;

<sup>4</sup> Inner Mongolia Water Resource Protection and Utilization Key Laboratory, Water Conservancy  
and Civil Engineering College, Inner Mongolia Agricultural University, Hohhot 010021, China

**Corresponding author:** Ruihong Yu (rhyu@imu.edu.cn) and Tingxi Liu ([txliu@imau.edu.cn](mailto:txliu@imau.edu.cn))

**Abstract:** Gradual riparian wetland drying is increasingly sensitive to global warming and contributes to climate change. Riparian wetlands play a significant role in regulating carbon and nitrogen cycles. In this study, we analyzed the emissions of carbon dioxide (CO<sub>2</sub>), methane (CH<sub>4</sub>), and nitrous oxide (N<sub>2</sub>O) from riparian wetlands in the Xilin River Basin to understand the role of these ecosystems in greenhouse gas (GHG) emissions. Moreover, the impact of the catchment hydrology and soil property variations on GHG emissions over time and space were evaluated. Our results demonstrate that riparian wetlands emit larger amounts of CO<sub>2</sub> (335–2790 mg·m<sup>-2</sup>·h<sup>-1</sup> in the wet season and 72–387 mg·m<sup>-2</sup>·h<sup>-1</sup> in the dry season) than CH<sub>4</sub> and N<sub>2</sub>O to the atmosphere due to high plant and soil respiration. The results also reveal clear seasonal variations and spatial patterns along the transects in the longitudinal direction. N<sub>2</sub>O emissions showed a spatiotemporal pattern similar to that of CO<sub>2</sub> emissions. Near-stream sites were the only sources of CH<sub>4</sub> emissions, while the other sites served as sinks for these emissions. Soil moisture content and soil temperature were the essential factors controlling GHG emissions, and abundant aboveground biomass promoted the CO<sub>2</sub>, CH<sub>4</sub>, and N<sub>2</sub>O emissions. Moreover, compared to different types of grasslands, riparian wetlands were the potential hotspots of GHG emissions in the Inner Mongolian region. Degradation of downstream wetlands has reduced the soil carbon pool by approximately 60%, decreased CO<sub>2</sub> emissions by approximately 35%, and converted the wetland

from a CH<sub>4</sub> and N<sub>2</sub>O source to a sink. Our study showed that anthropogenic activities have extensively changed the hydrological characteristics of the riparian wetlands and might accelerate carbon loss, which could further affect GHG emissions.

**Keywords:** Riparian wetlands, Grasslands, Greenhouse gas, Spatial-temporal distribution, Impact factor, Xilin River Basin

## 1. Introduction

With the increasing rate of global warming, the change in the concentrations of greenhouse gases (GHGs) in the atmosphere is a source of concern in the scientific community (Cao et al., 2005). According to the World Meteorological Organization (WMO, 2018), the concentrations of carbon dioxide (CO<sub>2</sub>), methane (CH<sub>4</sub>), and nitrous oxide (N<sub>2</sub>O) in the atmosphere have increased by 146%, 257%, and 122%, respectively, since 1750. Despite their lower atmospheric concentrations, CH<sub>4</sub> and N<sub>2</sub>O absorb infrared radiation approximately 28 and 265 times more effectively at centennial timescales than CO<sub>2</sub> (IPCC, 2013), respectively. On a global scale, CO<sub>2</sub>, CH<sub>4</sub>, and N<sub>2</sub>O together are responsible for 87% of the GHG effect (Ferrón et al., 2007).

Wetlands are unique ecosystems that serve as transition zones between terrestrial and aquatic ecosystems. They play an important role in the global carbon cycle (Beger et al., 2010; Naiman and Decamps, 1997). Wetlands are sensitive to hydrological changes, particularly in the context of global climate change (Cheng and Huang, 2016). Moreover, wetland hydrology is affected by local anthropogenic activities, such as the construction of reservoirs, resulting in gradual drying. Although wetlands cover only 4–6% of the terrestrial land surface, they contain approximately 12–24% of global terrestrial soil organic carbon (SOC), thus acting as carbon sinks. Moreover, they release CO<sub>2</sub>, CH<sub>4</sub>, and N<sub>2</sub>O into the atmosphere and serve as carbon sources (Lv et al., 2013). During plant photosynthesis, the amount of carbon accumulated is generally higher than the amount of CO<sub>2</sub> consumed (plant respiration, animal respiration, and microbial decomposition) in the wetland; thus, the net effect of the wetland is that of a carbon sink. Wetlands are increasingly recognized as an essential part of nature, given their simultaneous functions as carbon sources and

sinks. Excessive rainfall causes an expansion in wetland area and a sharp increase in soil moisture content, thus enhancing respiration, methanogenesis, nitrification, and denitrification rates (Mitsch et al., 2009). On the other hand, reduced precipitation or severe droughts decrease water levels, causing the wetlands to dry up. The accumulated carbon is released back into the atmosphere through oxidation. Due to the increasing impact of climate change and human activity, drying of wetlands has been widely observed in recent years (Liu et al., 2006); more than half of global wetlands have disappeared since 1900 (Mitsch and Gosselink, 2007), and this tendency is expected to continue in the future. The loss of wetlands may directly shift the soil environment from anoxic to oxic conditions, while modifying the CO<sub>2</sub> and CH<sub>4</sub> source and sink functions of wetland ecological systems (Waddington and Roulet, 2000; Zona et al., 2013).

The Xilin River Basin in China is characterized by a marked spatial gradient in soil moisture content. It is a unique natural laboratory that may be used to explore the close relationships between the spatiotemporal variations in hydrology and riparian biogeochemistry. Wetlands around the Xilin River play an irreplaceable role with regard to local climate control, water conservation, the carbon and nitrogen cycles, and husbandry (Gou et al., 2015; Kou, 2018). Moreover, the Xilin River region is subjected to seasonal alterations in precipitation and temperature regimes. Construction of the Xilin River Reservoir has resulted in highly negative consequences, such as the drying of downstream wetlands, thereby affecting riparian hydrology and microbial activity in riparian soils. GHG emissions in riparian wetlands vary immensely. Therefore, understanding the interactions between the GHG emissions and hydrological changes in the Xilin River riparian wetlands has become increasingly important. Moreover, it is necessary to estimate the changes in GHG emissions as a result of wetland degradation at local and global scales.

In this work, GHG emissions from riparian wetlands and adjacent hillslope grasslands of the Xilin River Basin were investigated. GHG emissions, soil temperature, and soil moisture content were measured in the dry and wet seasons. The main objectives of this study were to (1) investigate the temporal and spatial variations in CO<sub>2</sub>, CH<sub>4</sub>, and N<sub>2</sub>O emissions from the wetlands in the riparian zone, and examine the main factors affecting the GHG emissions; (2) compare the GHG emissions from the riparian wetlands with those from different types of grasslands; and (3) evaluate the impact of wetland degradation in the study area on GHG emissions.

## **2. Materials and methods**

### **2.1 Study site**

The Xilin River is situated in the southeastern part of the Inner Mongolia Autonomous Region in China (E115°00'–117°30', N43°26'–44°39'). It is a typical inland river of the Inner Mongolia grasslands. The river basin area is 10,542 km<sup>2</sup>, total length is 268.1 km, and average altitude is 988.5 m. According to the meteorological data provided by the Xilinhot Meteorological Station (Xi et al., 2017; Tong et al., 2004), the long-term annual mean air temperature is 1.7°C, and the maximum and minimum monthly means are 20.8°C in July and –19.8°C in January, respectively. The average annual precipitation was 278.9 mm for the period of 1968–2015. Precipitation is distributed unevenly among the seasons, with 87.41% of the total precipitation occurring between May and September.

Soil types in the Xilin River Basin are predominantly chernozems (86.4%), showing a significant zonal distribution as light chestnut soil, dark chestnut soil, and chernozems from the northwest to southeast. Soil types in this basin also present a vertical distribution with elevation. Soluble chernozems and carbonate chernozems are primarily observed at altitudes above 1,350 m, with a relatively fertile and deep soil layer. Dark chestnut soil, boggy soil, and dark meadow with high humus content are distributed between the altitudes of 1,150 and 1,350 m. Meanwhile, light chestnut soil, saline meadow soil, and meadow solonchak with low soil humus, a thin soil layer, and coarse soil texture are distributed between the altitudes of 902 and 1,150 m (Xi et al., 2017).

### **2.2 Field measurements and laboratory analyses**

In this study, five representative transects were selected as the primary measurement sites in the entire Xilin River. Each transect cuts through the riparian wetlands near the river and the hillslope grasslands further away (Fig. 1).

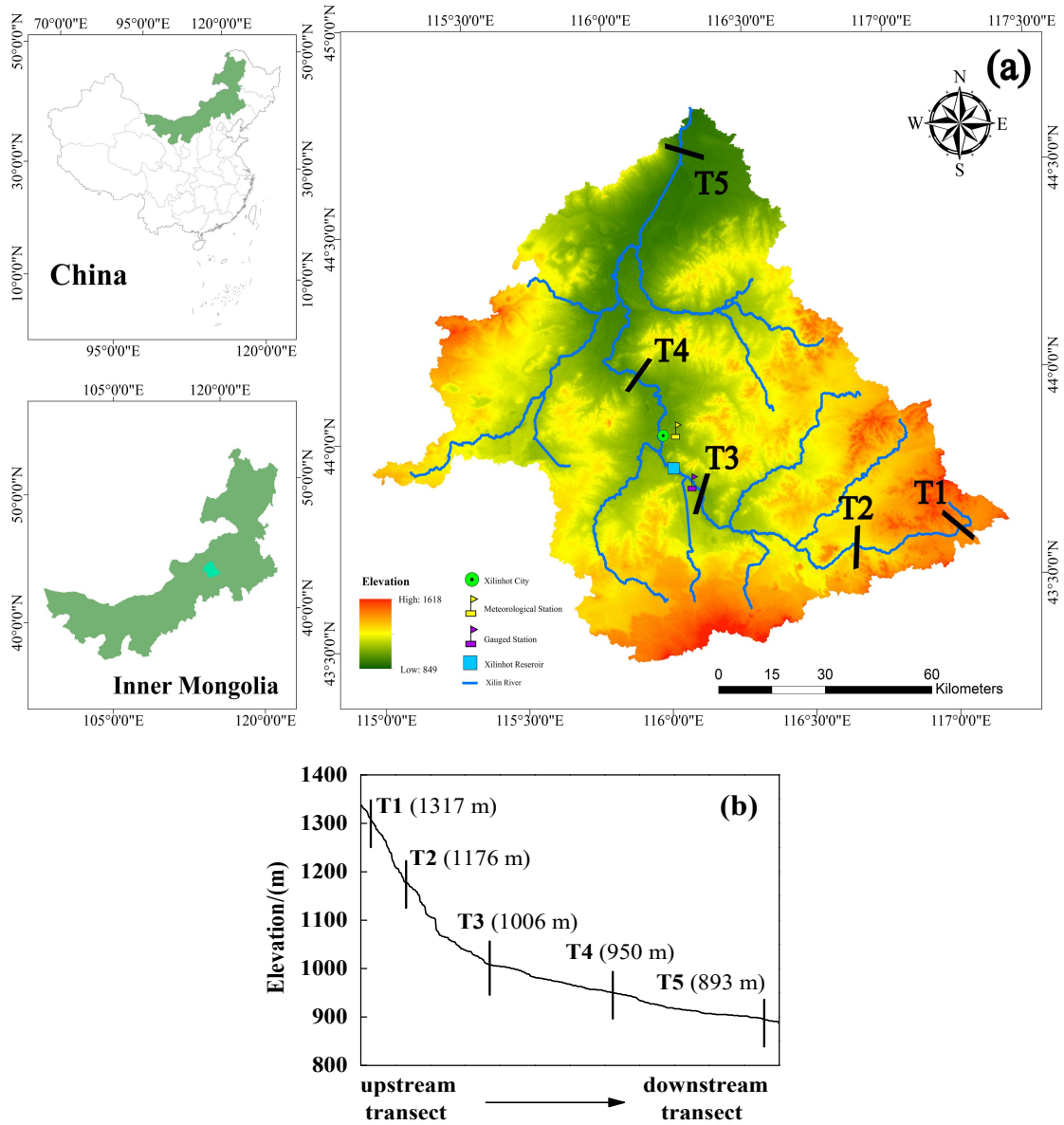


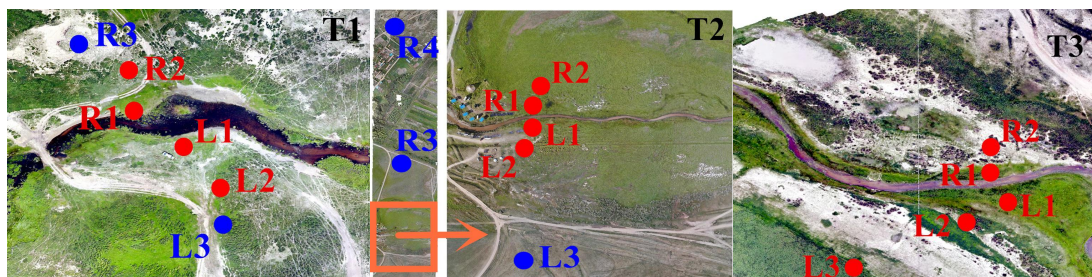
Fig. 1 (a) Location of the Xilin River Basin and distribution of five riparian-hillslope transects (T1–T5). (b) Elevation details of each transect in the Xilin River Basin.

The layout of the sampling points of each transect is shown in Fig. 2. Each sampling point, from T1–T5, was extended from either side of the river to the grassland on the slopes by using 5–7 sampling points for each transect, resulting in 24 points in total. The sampling sites on the left and right banks were defined as L1–L3 and R1–R4 from the riparian wetlands to the hillslope grasslands. As transect T3 was located on a much wider flood plain, none of its sampling points were located on the hillslope grassland. The last transect (T5) was located downstream in the dry lake and contained seven sampling points. They were defined as S1–S7, where S1, S2, and S7

were located along the lake shore (the lakeside zone), and S3–S6 were located in the dry lake bed (S3 and S4 in the mudbank, S5 in saline–alkali soil, and S6 in sand–gravel geology). Moreover, characterizations for the T1, T2, and T3 transects were located along the continuous river flow, and the T4 and T5 transects were located along the intermittent river flow.

The CO<sub>2</sub>, CH<sub>4</sub>, and N<sub>2</sub>O emissions from each site were measured in August (wet season) and October (dry season) in 2018 using a static dark chamber and the gas chromatography method. The static chambers were made of a cube-shaped polyvinyl chloride (PVC) pipe (dimensions: 0.4 m × 0.2 m × 0.2 m). A battery-driven fan was installed horizontally inside the top wall of the chamber to ensure proper air mixing during measurements. To minimize heating from solar radiation, white adiabatic aluminum foil was used to cover the entire aboveground portion of the chamber. During measurements, the chambers were driven into the soil to ensure airtightness and connected with a differential gas analyzer (Li-7000 CO<sub>2</sub>/H<sub>2</sub>O analyzer, LI-COR, USA) to measure the changes in the soil CO<sub>2</sub> concentration. The air in the chamber was sampled using a 60 mL syringe at 0, 7, 14, 21, and 28 min. The gas samples were stored in a reservoir bag and taken to the laboratory for CH<sub>4</sub> and N<sub>2</sub>O measurements using gas chromatography (GC-2030, Japan). The measurements were scheduled for 9:00–11:00 a.m. or 3:00–5:00 p.m.

Soil temperature (ST) was measured at depths of 0–10 cm and 10–20 cm with a geothermometer (DTM-461, Hengshui, China). Plant samples were collected in a static chamber and oven-dried in the laboratory to obtain aboveground biomass (BIO). A 100 cm<sup>3</sup> ring cutter was used to collect surface soil samples at each site, which were placed in aluminum boxes and immediately brought back to the laboratory to measure soil mass moisture content (SMC) and soil bulk density ( $\rho_b$ ) using national standard methods (NATESC, 2006). Topsoil samples were collected, sealed in plastic bags, and brought back to the laboratory to measure soil pH, electrical conductivity (EC), total soil organic carbon (TOC) content, and soil C:N ratio.



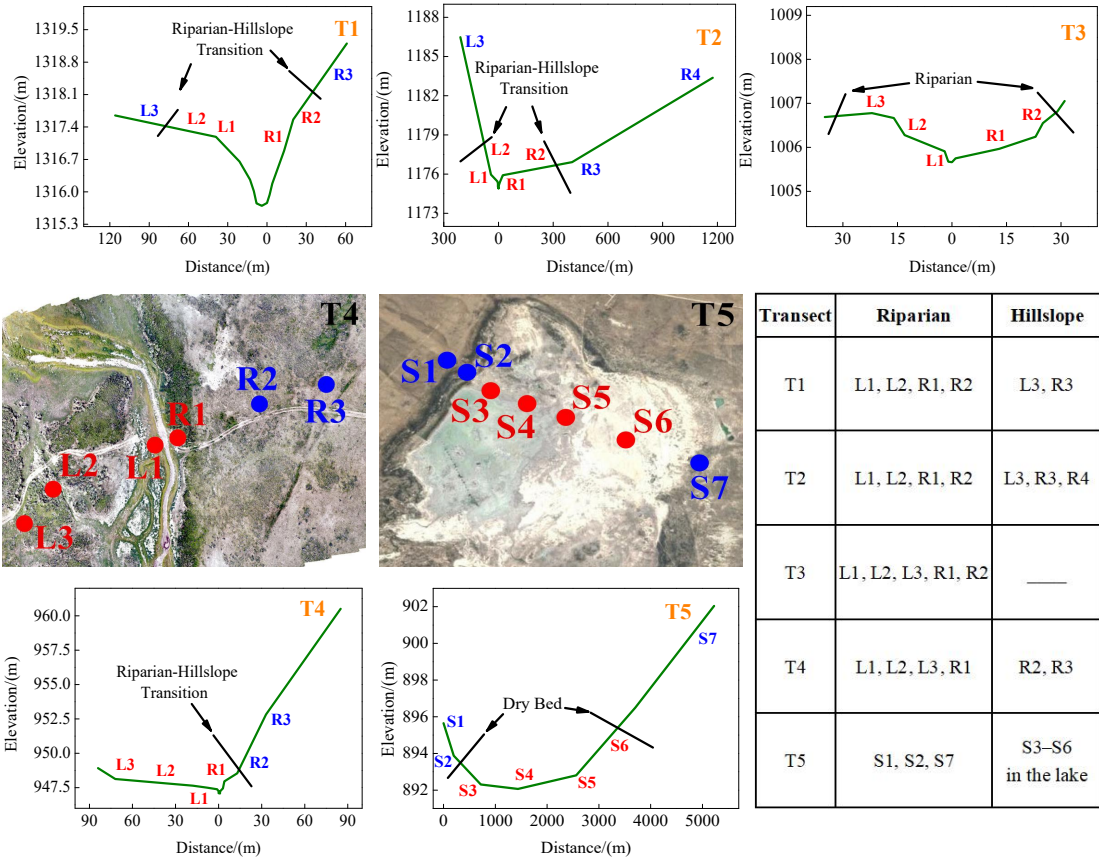


Fig. 2 Distributions of sampling points in transects T1–T5 (The images are authors' own)

Table 1. Physical and chemical properties (Mean  $\pm$  SD) of soils at various sites within each

transect

Trans ect	Sampl e		SMC10-V	SMC20-V	Soil C:N	TOC (g·kg <sup>-1</sup> )	BIO (g)	$\rho_b$	pH	EC (μs/cm)	SSM (%)
	Zone	numb er									
T1	Riparian	12	12.16 $\pm$ 7.55	12.88 $\pm$ 12.05	12.46 $\pm$ 0.91	30.16 $\pm$ 6.54	14.67 $\pm$ 5.44	1.28 $\pm$ 0.07	7.25 $\pm$ 0.62	154.71 $\pm$ 23.70	47.77 $\pm$ 7.04
	Hillslope	6	2.72 $\pm$ 0.91	5.05 $\pm$ 3.09	11.41 $\pm$ 0.09	10.77 $\pm$ 4.72	6.70 $\pm$ 1.48	1.45 $\pm$ 0.03	7.22 $\pm$ 0.40	82.02 $\pm$ 16.37	31.02 $\pm$ 1.32
T2	Riparian	12	26.75 $\pm$ 19.52	12.19 $\pm$ 7.82	11.70 $\pm$ 1.14	19.96 $\pm$ 5.71	24.76 $\pm$ 9.65	1.23 $\pm$ 0.05	8.95 $\pm$ 0.45	303.88 $\pm$ 102.16	51.21 $\pm$ 6.49
	Hillslope	9	5.85 $\pm$ 4.82	3.03 $\pm$ 1.43	9.77 $\pm$ 0.88	14.87 $\pm$ 11.21	6.10 $\pm$ 3.19	1.38 $\pm$ 0.13	8.10 $\pm$ 0.55	162.97 $\pm$ 128.18	35.09 $\pm$ 6.75
T3	Riparian	12	28.04 $\pm$ 22.95	14.53 $\pm$ 8.98	15.80 $\pm$ 4.16	22.40 $\pm$ 9.69	6.37 $\pm$ 2.95	1.35 $\pm$ 0.19	9.50 $\pm$ 0.67	1233.20 $\pm$ 829.83	47.56 $\pm$ 11.65
	L3	3	116.37 $\pm$	113.36 $\pm$	16.8 $\pm$	36.1 $\pm$	107.75	0.592 $\pm$	8.5 $\pm$	403 $\pm$ 57.21	>100

			56.91	23.17	0.58	1.84	±16.94	0.02	0.17		
					12.52 ±	9.96 ±	11.97 ±	1.30 ±	8.84 ±	461.72 ±	44.08 ±
	Riparian	12	5.42 ± 3.34	4.07 ± 4.31	2.06	1.25	4.50	0.08	0.22	314.27	7.07
T4					9.97 ±	9.65 ±		1.30 ±	8.23 ±		39.43 ±
	Hillslope	6	3.35 ± 2.06	4.27 ± 1.94	0.50	1.05	7.84 ± 2.48	0.09	0.14	118.5 ± 8.25	5.55
	Dry lake	12	17.47 ±	14.49 ±	63.74 ±	31.41 ±	5.48 ± 2.35	1.16 ±	9.88 ±	7320.87 ±	58.47 ±
	bed		15.08	13.28	12.93	6.55		0.10	0.18	4300.03	7.16
T5					15.92 ±	6.35 ±		1.33 ±	9.41 ±	281.82 ±	37.52 ±
	Lake	9	2.64 ± 1.48	2.82 ± 1.27	4.71	1.16	0	0.09	0.7	162.73	5.34
	shore										

Note: SMC10-V - soil volumetric moisture content in 0-10 cm; SMC20-V - soil volumetric moisture content in 10-20 cm; Soil C:N - soil carbon-nitrogen ratio; TOC - total soil organic carbon; BIO - aboveground biomass;  $\rho_b$  - soil bulk density; pH - soil pH; EC - soil electrical conductivity; SSM - saturated soil moisture.

Table 2. Soil particle composition of soils at various sites within each transect

Transect	Zone	Soil particle composition		
		Clay %	Silt %	Sand
		(<0.002 mm)	(0.02~0.002 mm)	(2.0 ~0.02 mm)
T1	Riparian	2.5	2.7	94.8
	Hillslope	9.6	6.1	85.3
T2	Riparian	5.5	5.8	90.7
	Hillslope	10.8	8.6	80.6
T3	Riparian	4.1	1.1	94.8
T4	Riparian	11.4	1.5	87.1
	Hillslope	12.7	5.9	81.4
T5	Lake shore	5.1	2.1	92.8
	Dry lake bed	46.1	4.8	49.1

## 2.3 Calculation of GHG emissions

The CO<sub>2</sub>, CH<sub>4</sub>, and N<sub>2</sub>O emissions were calculated using Eq. 1 (Qin et al., 2016):

$$F = \frac{V}{A} \times \frac{dc}{dt} \times \rho = H \times \frac{dc}{dt} \times \frac{M}{V} \times \left( \frac{273.15}{273.15 + t} \right) \quad (1)$$

Where  $F$  denotes the flux of CO<sub>2</sub>, CH<sub>4</sub>, and N<sub>2</sub>O emissions (mg·m<sup>-2</sup>·h<sup>-1</sup>),  $H$  is the height of the static chamber (0.18 m),  $M$  is the relative molecular weight (44 for CO<sub>2</sub> and N<sub>2</sub>O, and 16 for CH<sub>4</sub>),  $V$  is the volume of gas in the standard state (22.4 L·mol<sup>-1</sup>),  $dc/dt$  is the rate of change of the gas concentration (10<sup>-6</sup>·h<sup>-1</sup>), and  $T$  is the temperature in the black chamber (°C).



The annual cumulative emissions were calculated using Eq. 2 (Whiting G and Chanton J., 2001):

$$M = \sum \frac{F_{i+1} + F_i}{2} \times (t_{i+1} - t_i) \times 24 \quad (2)$$

Where M denotes the total cumulative emission amounts of CO<sub>2</sub>, CH<sub>4</sub>, or N<sub>2</sub>O (kg·hm<sup>2</sup>), F is the emission flux of CO<sub>2</sub>, CH<sub>4</sub>, or N<sub>2</sub>O, i is the sampling frequency, and t<sub>i+1</sub>-t<sub>i</sub> represents the interval between two adjacent measurement dates.

In this study, a 100-year scale was selected to calculate the global warming potential (GWP) of soil CH<sub>4</sub> and N<sub>2</sub>O emissions (Whiting G and Chanton J., 2001):

$$GWP = 1 \times [CO_2] + 25 \times [CH_4] + 298 \times [N_2O] \quad (3)$$

Where 25 and 298 are the GWP multiples of CH<sub>4</sub> and N<sub>2</sub>O relative to CO<sub>2</sub> on a 100-year time scale, respectively.

## 2.4 Statistical Analysis

All statistical analyses were performed using SPSS for Windows version 18.0 (SPSS Inc., Chicago, IL, USA). Statistical significance was set at P < 0.05. Pearson correlation analysis was conducted to estimate the relationships between GHG fluxes and environmental variables. A Wilcoxon test was used to determine the differences in the GHG fluxes between the two seasons.

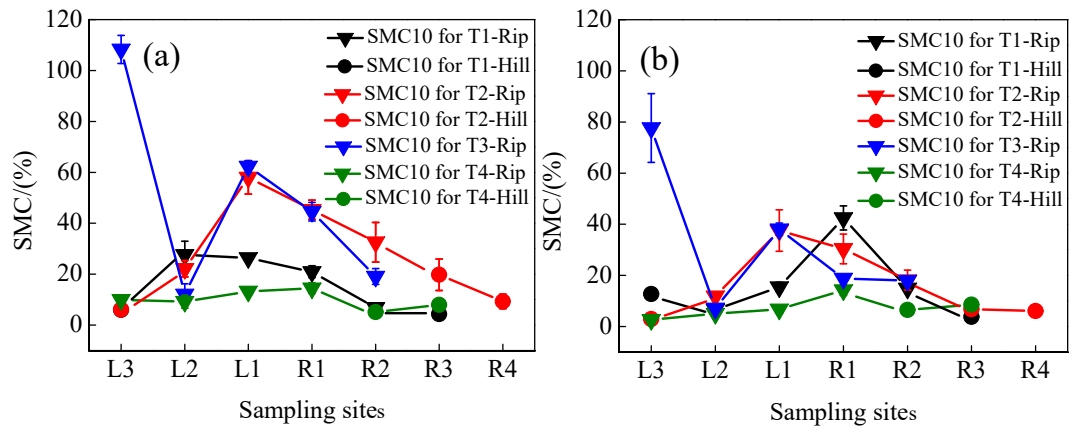
## 3. Results

### 3.1 Spatiotemporal patterns of SMC for each transect

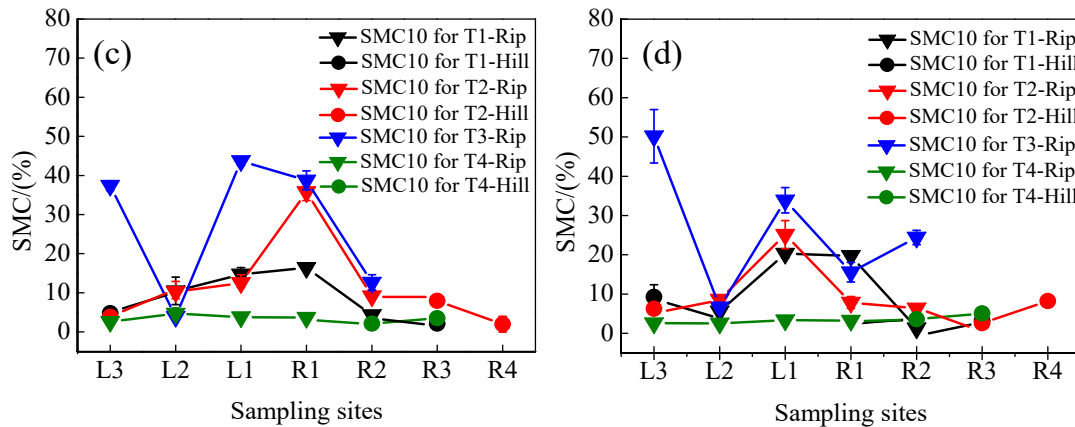
The temporal and spatial variations in SMC10 occurred in the following order: wet season > dry season and riparian wetlands > hillslope grasslands (Fig. 3a, c, e). Similar variations were observed in SMC20 (Fig. 3b, d, f). The average SMC10 and SMC20 in the continuous river transects in the riparian zones (SMC10 values were 37.44% in the wet season and 19.40% in the dry season, while SMC20 values were 25.96% in the wet season and 17.39% in the dry season) were higher than those in the hillslope grasslands (SMC10 values were 9.12% in the wet season and 4.15% in the dry season; SMC20 values were 6.51% in the wet season and 5.96% in the dry season). During the study period, both SMC10 and SMC20 changed as the distance from the river increased, and the highest value was observed at the near-stream sites (L1 and R1). SMC10 fluctuations were low in the intermittent transect compared with those in the upstream transects,

with mean values being 11.79% in the wet season and 3.72% in the dry season in the riparian areas. The mean SMC10 in the hillslopes was 6.58% in the wet season and 2.86% in the dry season. SMC20 showed similar fluctuation; it was 7.22% in the wet season and 2.98% in the dry season in the riparian areas, and 7.56% in the wet season and 4.4% in the dry season in the hillslopes. In transect T5, average SMC10 and SMC20 at the center of the lake (SMC10 values were 29.00% in the wet season and 13.36% in the dry season; SMC20 values were 29.30% in the wet season and 9.69% in the dry season) were higher than those along the lake shore (SMC10 values were 4.90% in the wet season and 3.13% in the dry season; SMC20 values were 3.34% in the wet season and 5.22% in the dry season).

Wet season



Dry season



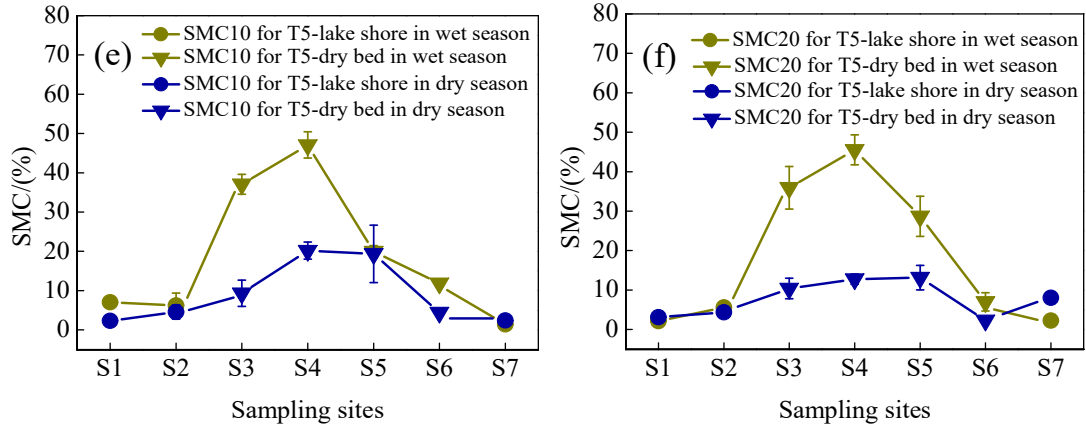
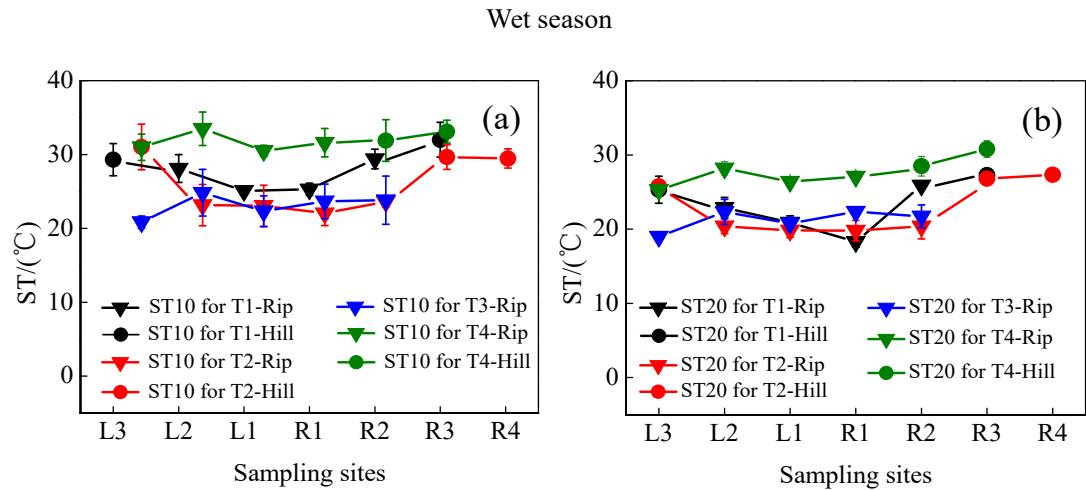


Fig. 3 Soil mass moisture contents (SMCs) at soil depths of 0–10 cm (SMC10) and 10–20 cm (SMC20) for transects T1–T5 in the wet and dry seasons. Error bars represent the SD about the mean.

### 3.2 Spatiotemporal patterns of ST in each transect

Spatiotemporal differences in ST during the entire observation period are displayed in Fig. 4. ST variations in the wet season (mean, 27.4 °C) were noticeably higher than those in the dry season (mean, 8.97 °C). Moreover, ST at riparian sites (mean, 26.0 °C in the wet season and 8.41 °C in the dry season) was slightly lower than that at the hillslope grasslands (mean, 30.9 °C in the wet season and 10.3 °C in the dry season) for the 0–10 cm soil depth, with the exception of transect T5. Similar results were observed for the 10–20 cm soil depth.



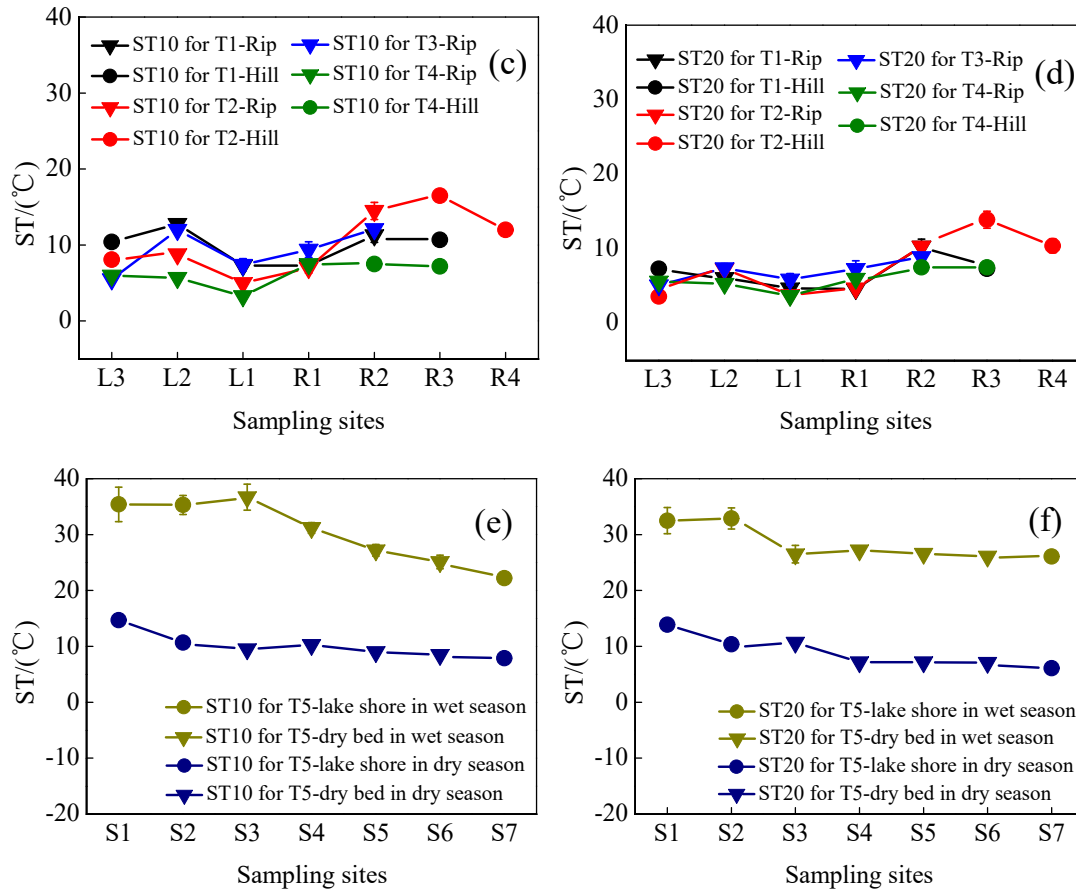


Fig. 4 Soil temperatures (STs) at soil depths of 0–10 cm (ST10) and 10–20 cm (ST20) for transects T1–T5 in the wet and dry seasons. Error bars represent the SD about the mean.

### 3.3 Spatiotemporal patterns of GHG emissions in each transect

Figure 5 shows the spatiotemporal variations in GHG emissions in the wet and dry seasons in each transect. CO<sub>2</sub> emissions in each transect were higher in the wet season than in the dry season. The average emissions in the riparian wetland transects T1–T4 ( $1582.09 \pm 679.34 \text{ mg} \cdot \text{m}^{-2} \cdot \text{h}^{-1}$  in the wet season and  $163.24 \pm 84.98 \text{ mg} \cdot \text{m}^{-2} \cdot \text{h}^{-1}$  in the dry season) were higher than the transects in the hillslope grasslands ( $1071.54 \pm 225.39 \text{ mg} \cdot \text{m}^{-2} \cdot \text{h}^{-1}$  in the wet season and  $77.68 \pm 25.32 \text{ mg} \cdot \text{m}^{-2} \cdot \text{h}^{-1}$  in the dry season). High CO<sub>2</sub> fluxes occurred in the riparian zones, while lower CO<sub>2</sub> fluxes were observed in the hillslope grasslands in continuous river transects (T1, T2, and T3). Transect T4 exhibited lower CO<sub>2</sub> emission in the riparian wetlands near the channel than at sites away from the channel. CO<sub>2</sub> emissions in transect T5 in the wet and dry seasons decreased from the lake shore to the lake center.

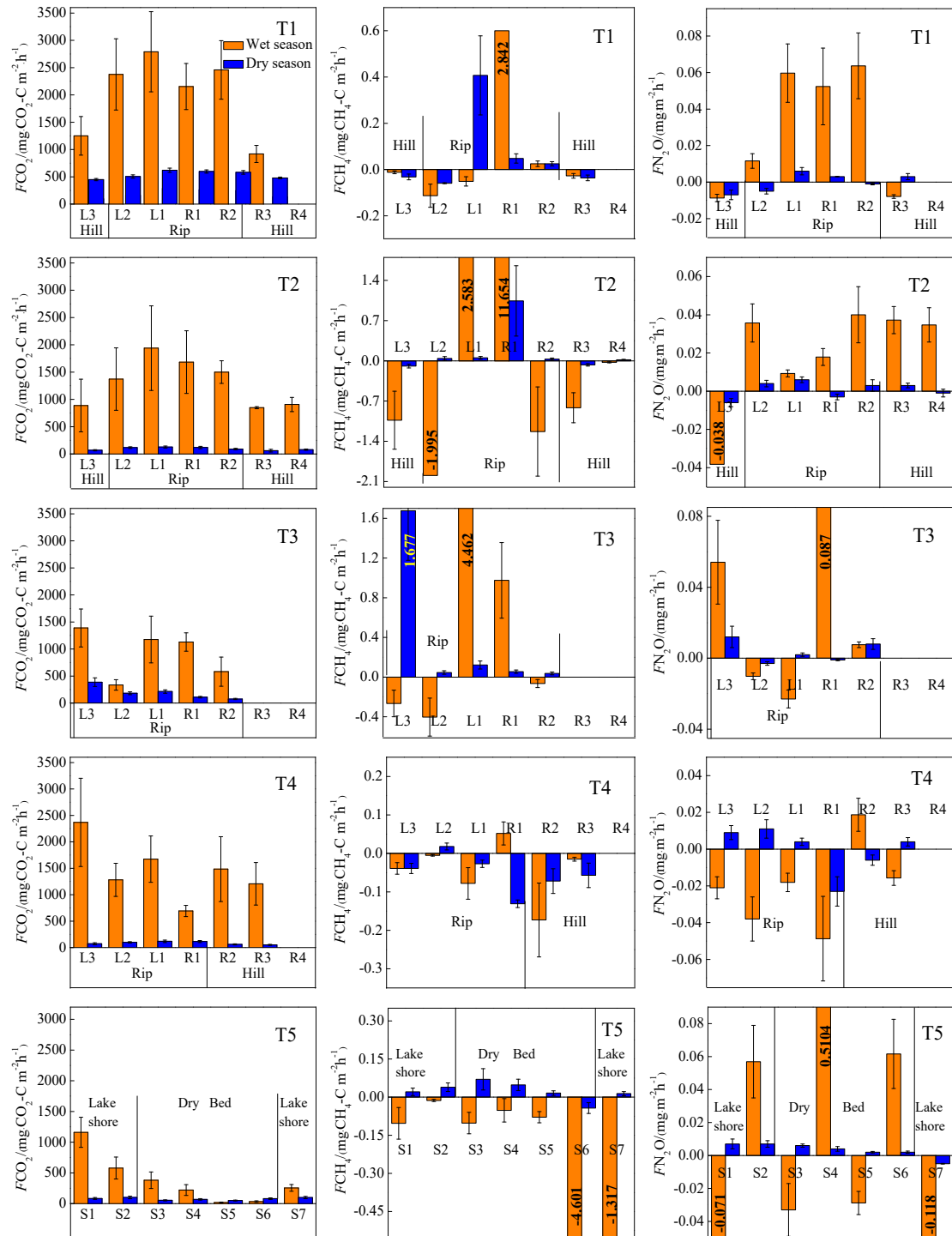


Fig. 5 Spatiotemporal patterns of CO<sub>2</sub> (first column), CH<sub>4</sub> (second column), and N<sub>2</sub>O

(third column) emission ( $F$ ) for each transect. Data are shown for the wet season (orange) and the dry season (blue). Error bars depict standard deviation.

CH<sub>4</sub> emissions at the continuous river flow transects (T1, T2, and T3) varied between the wet and dry seasons, except for those at T4 (characterized by intermittent river flow) and T5 (the dry

lake). In the wet season, the near-stream sites (L1 and R1) in T1, T2, and T3 were characterized as high CH<sub>4</sub> sources (average,  $3.74 \pm 3.81 \text{ mg} \cdot \text{m}^{-2} \cdot \text{h}^{-1}$ ), but the sites located away from the river gradually turned into CH<sub>4</sub> sinks. Moreover, all the sites in transects T4 and T5 were sinks. CH<sub>4</sub> emissions (mean value:  $0.2 \pm 0.45 \text{ mg} \cdot \text{m}^{-2} \cdot \text{h}^{-1}$ ) at the wetland sites were always lower in the dry season than those in the wet season. However, the sites on the hillslope grasslands served as CH<sub>4</sub> sinks (mean value:  $-0.05 \pm 0.03 \text{ mg} \cdot \text{m}^{-2} \cdot \text{h}^{-1}$ ). In transect T5, CH<sub>4</sub> emissions showed the opposite trend; a CH<sub>4</sub> sink was observed in the wet season, but it was transformed into a CH<sub>4</sub> source in the dry season.

Similar to the CO<sub>2</sub> and CH<sub>4</sub> emissions, N<sub>2</sub>O emissions showed a distinct spatiotemporal pattern in all the transects. N<sub>2</sub>O emissions in the wet season were higher than those in the dry season. These emissions were higher in the riparian wetlands than in the hillslope grasslands. Moreover, almost all sites with continuous river flow were N<sub>2</sub>O sources, while more than half of the sites with intermittent river flow were sinks.

Table 3 shows that CO<sub>2</sub> fluxes were significantly correlated between the wet and dry seasons, while CH<sub>4</sub> and N<sub>2</sub>O fluxes were not correlated between the two seasons.

Table 3 Significant correlations between GHGs fluxes and two seasons (n=31)

GHG flux	FCO <sub>2</sub> in the wet season - FCO <sub>2</sub> in the dry season	FCH <sub>4</sub> in the wet season - FCH <sub>4</sub> in the dry season	FN <sub>2</sub> O in the wet season - FN <sub>2</sub> O in the dry season
Significant correlations (P)	0.000	0.133	0.290

Note:  $P < 0.05$  denotes significant correlation and  $P > 0.05$  denotes no significant correlation

### 3.4 Spatiotemporal patterns of GHG emission in upstream and downstream areas

Figure 6 shows the detailed spatial and seasonal patterns of GHG emission in the wet and dry seasons in the longitudinal direction from the upstream (T1, T2, and T3) to the downstream areas (T4 and T5). The CO<sub>2</sub>, CH<sub>4</sub>, and N<sub>2</sub>O emissions were calculated using the average values of the respective emissions in the wetlands and hillslope grasslands in each transect.

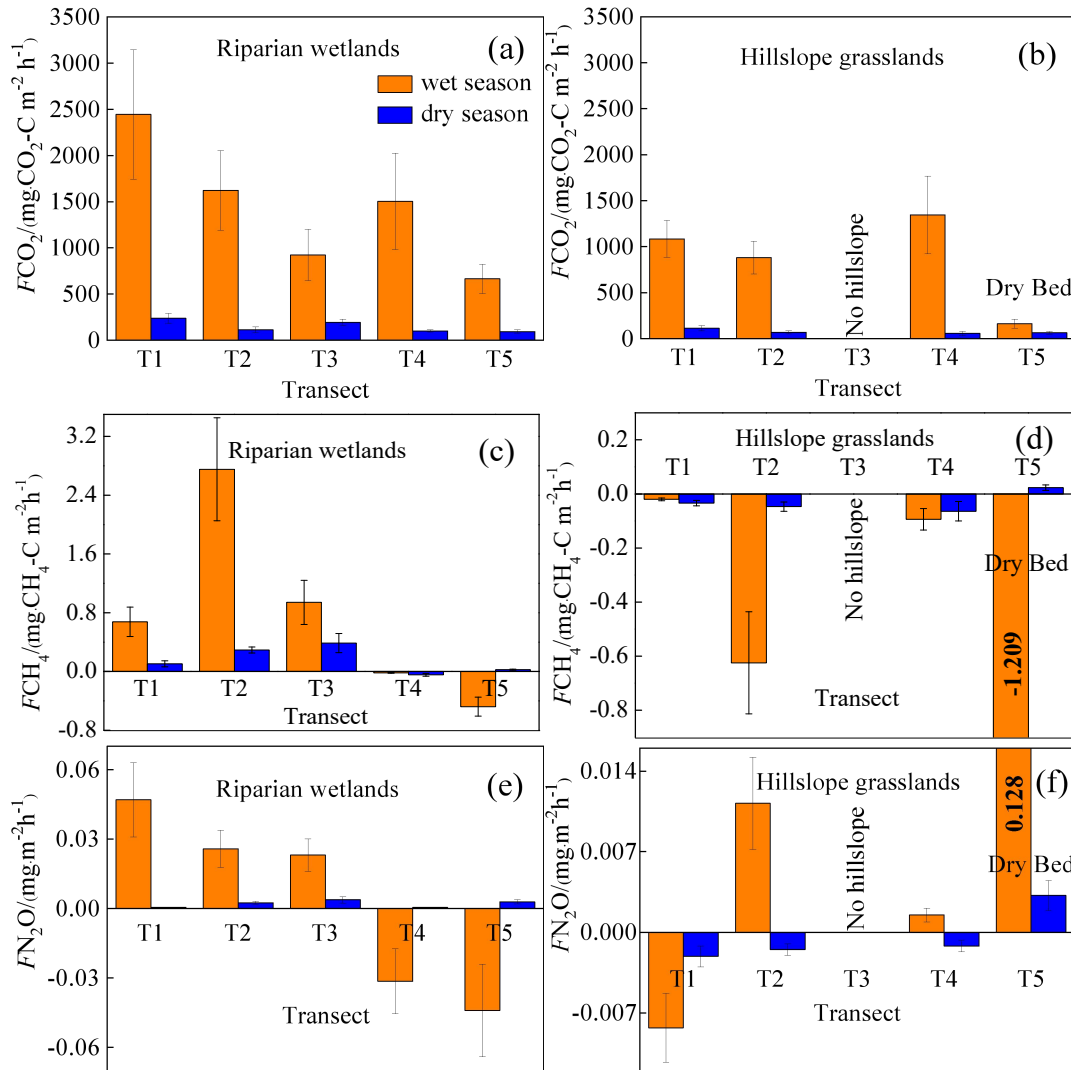


Fig. 6 Spatiotemporal patterns of CO<sub>2</sub> (first line), CH<sub>4</sub> (second line), and N<sub>2</sub>O (third line) emissions ( $F$ ) in the upstream (T1, T2, and T3) and downstream areas (T4 and T5). Bars represent the mean values for each transect and error bars show the standard errors.

CO<sub>2</sub> emissions at the riparian wetlands (Fig. 6(a)) in the wet season decreased from  $2,444.69 \pm 228.58 \text{ mg} \cdot \text{m}^{-2} \cdot \text{h}^{-1}$  in the upstream area to  $665.08 \pm 347.57 \text{ mg} \cdot \text{m}^{-2} \cdot \text{h}^{-1}$  downstream, and the corresponding values for the dry season were  $238.12 \pm 48.20 \text{ mg} \cdot \text{m}^{-2} \cdot \text{h}^{-1}$  and  $94.14 \pm 7.67 \text{ mg} \cdot \text{m}^{-2} \cdot \text{h}^{-1}$ , respectively. However, in the hillslope grasslands (Fig. 6(b)), CO<sub>2</sub> emissions exhibited no significant seasonality between the upstream and downstream areas, with mean values being  $1,103.40 \pm 190.44 \text{ mg} \cdot \text{m}^{-2} \cdot \text{h}^{-1}$  in the wet season and  $79.18 \pm 24.52 \text{ mg} \cdot \text{m}^{-2} \cdot \text{h}^{-1}$  in the dry season. In addition, the CO<sub>2</sub> emissions in transect T5 were low for both months, with the averages of  $162.83 \pm 149.15 \text{ mg} \cdot \text{m}^{-2} \cdot \text{h}^{-1}$  and  $63.26 \pm 12.40 \text{ mg} \cdot \text{m}^{-2} \cdot \text{h}^{-1}$  in the wet and dry season,

respectively. The upstream riparian zones exhibited higher CO<sub>2</sub> emissions ( $894.32 \pm 868.47$  mg·m<sup>-2</sup>·h<sup>-1</sup>) than their downstream counterparts ( $621.14 \pm 704.10$  mg·m<sup>-2</sup>·h<sup>-1</sup>). Mean CO<sub>2</sub> emissions showed no significant differences in the grasslands, averaging  $524.16 \pm 450.10$  mg·m<sup>-2</sup>·h<sup>-1</sup> upstream and  $508.06 \pm 534.77$  mg·m<sup>-2</sup>·h<sup>-1</sup> downstream.

CH<sub>4</sub> emissions showed a marked spatial pattern in the riparian zones from upstream to downstream (Fig. 6(c)). The transects with continuous river flow were CH<sub>4</sub> sources in the wet and dry seasons, with average emissions of  $1.42 \pm 3.41$  mg·m<sup>-2</sup>·h<sup>-1</sup> and  $0.27 \pm 0.49$  mg·m<sup>-2</sup>·h<sup>-1</sup>, respectively; while those with intermittent river flow served as CH<sub>4</sub> sinks, with the corresponding means of  $-0.21 \pm 0.45$  mg·m<sup>-2</sup>·h<sup>-1</sup> and  $-0.02 \pm 0.05$  mg·m<sup>-2</sup>·h<sup>-1</sup>, respectively. Moreover, the hillslope grassland sites in all transects were CH<sub>4</sub> sinks (Fig. 6(d)).

N<sub>2</sub>O emissions in riparian wetlands (Fig. 7(e)) showed spatial patterns similar to those of CH<sub>4</sub> emissions. In the wet season, the transects with continuous river flow served as N<sub>2</sub>O sources, with a mean emission of  $0.031 \pm 0.031$  mg·m<sup>-2</sup>·h<sup>-1</sup>; meanwhile, transects with intermittent river flow acted as N<sub>2</sub>O sinks with an average emission of  $-0.037 \pm 0.05$  mg·m<sup>-2</sup>·h<sup>-1</sup>. In the dry season, N<sub>2</sub>O emissions occurred as weak sources in the longitudinal transects, exhibiting an average emission of  $0.002 \pm 0.007$  mg·m<sup>-2</sup>·h<sup>-1</sup>. However, the N<sub>2</sub>O emission in the hillslope grasslands did not show any spatial patterns (Fig. 7(f)).

## **4. Discussion**

### **4.1 Main factors influencing GHG emissions**

#### **4.1.1 Effects of SMC on GHG emissions**

SMC constitutes one of the main factors affecting GHG emission in wetlands. In this study, transects T1–T4 were characterized by a marked spatial SMC gradient (i.e., a gradual decrease in SMC10 and SMC20 from the riparian wetlands to the hillslope grasslands and from the upstream to downstream regions (Fig. 3)). The CO<sub>2</sub>, CH<sub>4</sub>, and N<sub>2</sub>O emissions showed a similar trend. Table 4 shows that SMC10 is positive correlated with CO<sub>2</sub> emission ( $P < 0.05$ ), and that SMC10 and SMC20 are significantly positively correlated with CH<sub>4</sub> emission ( $P < 0.01$ ) and with N<sub>2</sub>O emission ( $P < 0.05$  and  $P < 0.01$ , respectively). These results indicate the influence of wetland SMC on GHG emission.

Typically, the optimal SMC associated with CO<sub>2</sub> emission in the riparian wetlands ranges from 40 to 60% (Sjögersten et al., 2006), creating better soil aeration, and improving soil



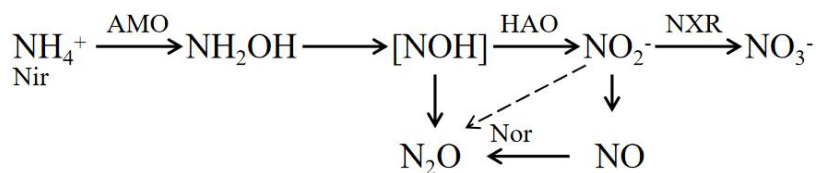
microorganism activity and respiration in plant roots, thereby promoting CO<sub>2</sub> emission. Excessive SMC reduces soil gas transfer due to the formation of an anaerobic environment in the soil, and microbial activity is lowered, favoring the accumulation of organic matter (Hui., 2014). The SMC of the hillslope grasslands was found to be less than 10%. Low soil moisture inhibits the growth of vegetation, with few vegetation residues and litters. Meanwhile, low soil moisture is not conducive to the survival of soil microorganisms, leading to lower CO<sub>2</sub> emission from the hillslope grasslands than from the riparian zones (Moldrup et al., 2000; Hui., 2014). Similar results were obtained in our study. The change in CO<sub>2</sub> emission in transect T5 was contrary to the changes in SMC10 and SMC20, likely because the optimal range of soil C:N is between 10-12 (Pierzynski et al., 1994), but the value in the dry lake bed of T5 is higher than 60. The high soil C:N resulted in nitrogen limitation in the process of decomposition of organic matter by microorganisms. Further, other sediment properties (like Soil pH > 9.5) for this transect were not conducive to the survival of microorganisms (Table 1), and the increase in SMC did not increase the respiration activity of the microorganisms.

The highest CH<sub>4</sub> emissions were observed at the near-stream sites (i.e., L1 and R1) in T1, T2, and T3, with average SMC of 30.29%, while the SMC at the other sites, which were either weak sources or sinks, averaged at 14.57%. These results indicate that a higher SMC is favorable for CH<sub>4</sub> emissions. This may be because a higher SMC accompanies soil in a reduced state, which is beneficial for CH<sub>4</sub> production and inhibits CH<sub>4</sub> oxidation. A similar result was reported by Xu et al. (2008). They conducted experiments analyzing CH<sub>4</sub> emissions from a variety of paddy soils in China, and showed that CH<sub>4</sub> production rates increased with the increase in SMC at the same incubation temperature. Meng et al. (2001) also reported that water depth was the main factor affecting CH<sub>4</sub> emissions from wetlands. When the water level dropped below the soil surface, the decomposition of organic matter accelerated, and CH<sub>4</sub> emission decreased. If the oxide layer is large, the soil is transformed into a CH<sub>4</sub> sink (Meng et al., 2011).

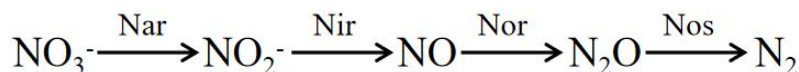
The N<sub>2</sub>O fluxes showed a clear spatial pattern associated with the changes in SMC. The moisture content of wetland soils directly affects the aeration status of the soil. Besides, the aeration status affects the partial pressure of oxygen, which has an important impact on nitrifying/denitrifying bacterial activity and ultimately affects soil N<sub>2</sub>O emissions (Zhang et al., 2005). Table 4 shows that N<sub>2</sub>O emission is significantly positively correlated with SMC10 and

SMC20 ( $P < 0.01$ ). Generally, when SMC is below the saturated water content, the microorganisms are in an aerobic environment, and  $N_2O$  mainly comes from the nitrification reaction.  $N_2O$  emission increases with increase in SMC (Niu et al., 2017; Yu et al., 2006). In our study, the sampling sites with higher SMC (riparian zones and some hillslope grassland zones in the upstream transects) have higher  $N_2O$  emissions. When SMC increases to the saturated water content or is in a flooded state, the system is an anaerobic environment, and the nitrous oxide reductase activity is higher due to excessively high SMC, which is conducive to denitrification and eventually produces  $N_2$  (Niu et al., 2017; Yu et al., 2006), such as at site L1 in transect T3 in this study. Ulrike et al. (2004) showed that denitrification was the main process under flooded soil conditions in wetland soils, and that the release of  $N_2$  exceeds that of  $N_2O$ . These findings are consistent with those of Liu et al. (2003), who showed that SMC is an essential factor affecting  $N_2O$  emission.

Nitrification:



Denitrification:



The enzymes involved in the formula include Ammonia monooxygenase (AMO), Hydroxylamine oxidase (HAO), Nitrite REDOX enzyme (HAO), nitrate reductase (Nar), nitrite reductase (Nir), Nitric oxide reductase (Nor), and Nitrous oxide reductase (Nos).

#### 4.1.2 Effects of ST on GHG emissions

ST was another important factor affecting  $CO_2$  emission in this study; it was found to be significantly correlated with  $CO_2$  emission ( $P < 0.01$ ) (Table 4). The activity of soil microorganisms increases with rising soil temperature, leading to increased respiration and consequently higher  $CO_2$  emission (Heilman et al., 1999). Previous studies have reported that ST partially controls seasonal  $CO_2$  emission patterns (Inubushi et al., 2003). Concurrently,  $CO_2$  emissions in the wet season were significantly higher than those in the dry season in this study.

$CH_4$  emissions showed a clear seasonal pattern, likely because high summer temperatures

improve the activity of both CH<sub>4</sub>-producing and -oxidizing bacteria (Ding et al., 2010). However, as Table 4 indicates, the correlation between CH<sub>4</sub> emission and temperature was not significant in this study, likely because SMC was a more critical factor than temperature in our study region given its very dry climate. SMC showed a positive correlation with GHG emissions. In addition, SMC affected ST to a certain extent, while the interactions between SMC and ST had a mutual influence on CH<sub>4</sub> emission. During the study period, the near-stream sites (L1 and R1) maintained a super-wet state on the ground surface for a long time, which was beneficial for the production of CH<sub>4</sub>. However, the wetlands maintained a state without water accumulation on the soil surface in August, which was conducive to the oxidative absorption of CH<sub>4</sub>. SMC thus masked the effect of ST on CH<sub>4</sub> emissions.

Previous studies have indicated that temperature is an important factor affecting N<sub>2</sub>O emission (Sun et al., 2011) through primary mechanisms impacting the nitrifying and denitrifying bacteria in the soil. As Table 4 shows, the correlations between N<sub>2</sub>O emission and ST10 and ST20 were poor ( $P > 0.05$ ). This can be attributed to the wide suitable temperature range for nitrification-denitrification and weak sensitivity to temperature. Malhi et al. (1982) found that the optimum temperature for nitrification was 20 °C, and that it inhibits entirely at 30 °C. However, Brady (1999) believed that the suitable temperature range for nitrification is 25~35 °C, and that nitrification inhibits below 5 °C or above 50 °C. This shows that the temperature requirements of nitrifying microorganisms in wetland soils are possibly different in different temperature belts. The suitable temperature range was the performance of the long-term adaptability of nitrifying microorganisms. Meanwhile, several studies have revealed that denitrification can be carried out in a wide temperature range (5~70 °C), and that it is positively related to temperature (Fan., 1995). However, the process is inhibited when the temperature is too high or too low. The average ST in the wet season was 27.4 °C, conducive to the growth of denitrifying microorganisms, while that in dry season was 8.97 °C, and the microbial activity was generally low (Sun et al., 2011). Furthermore, ST fluctuations were low both in the wet and dry seasons. Therefore, the effect of ST on N<sub>2</sub>O emission may have been masked by other factors, such as moisture content.

#### 4.1.3 Effects of BIO and soil organic matter content on GHG emissions

CO<sub>2</sub> and CH<sub>4</sub> emissions were higher in the riparian wetlands than in the grasslands, mainly because of the greater vegetation cover in the former. Typically, CO<sub>2</sub> emissions in the riparian

wetlands originate from plants and microorganisms, with plant respiration accounting for a large proportion in the growing season. Previous studies have shown that plant respiration accounts for 35–90% of the total respiration in the wetland ecosystem (Johnson-Randall and Foote, 2005). The good soil physicochemical properties and high soil TOC content of the riparian wetlands improve both the activity of soil microorganisms and plant root respiration. As Table 4 shows, BIO is significantly correlated with CO<sub>2</sub> ( $P < 0.05$ ) and CH<sub>4</sub> ( $P < 0.01$ ) emissions. These results are indicated by the significant linear positive correlation between the respiration rate and plant biomass (Lu et al., 2007). Higher plant biomass storage can achieve more carbon accumulation during photosynthesis and higher exudate release by the roots. This, in turn, promotes the accumulation of soil organic matter. Increased amount of organic matter stimulates the growth and reproduction of soil microorganisms, ultimately promoting CO<sub>2</sub> and CH<sub>4</sub> emission. Moreover, plants act as gas channels for CH<sub>4</sub> transmission, and a larger amount of biomass promotes CH<sub>4</sub> emission, given the increased number of channels. In transect T3, the high CO<sub>2</sub> emission observed at site L3 can be attributed to the relatively high levels of SMC, BIO, and soil nutrients, which stimulate microbial respiration rates.

BIO had a weak correlation with N<sub>2</sub>O emission (Table 4), which indicates that plants increase N<sub>2</sub>O production and emission, although this may not be the most critical factor. Previous studies have reported mechanisms wherein the plants are able to absorb the N<sub>2</sub>O produced in the soil through the root system before releasing it into the atmosphere. Additionally, the root exudates of plants can enhance the activity of nitrifying and denitrifying bacteria in the soil, ultimately promoting the production of N<sub>2</sub>O. Finally, oxygen stress caused by plant respiration can regulate the production and consumption of N<sub>2</sub>O in the soil, eventually affecting the conversion of nitrogen in the soil (Koops et al., 1996; Azam et al., 2005).

Site L3 in transect T3 was covered by tall reeds, and its BIO was much higher than that of any of the other sites; thus, the data for this site were excluded from the correlation analysis.

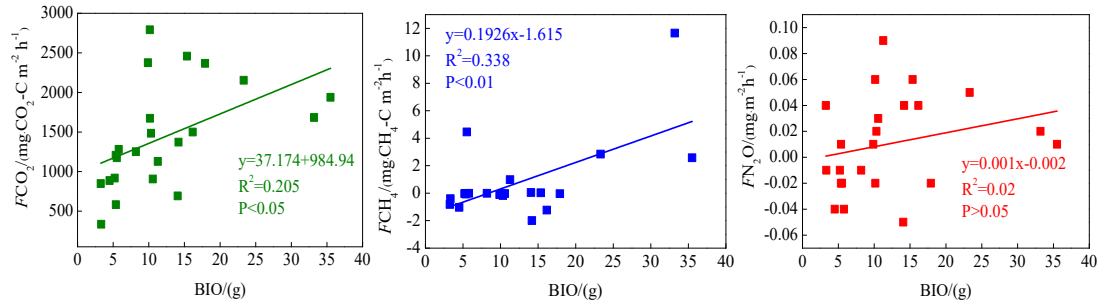


Fig. 7 Correlation between aboveground biomass (BIO) and GHG emission ( $F$ )

Soil C:N ratio refers to the ratio of the concentration biodegradable carbonaceous organic matter to nitrogenous matter in the soil, and it forms a soil matrix with TOC. TOC decomposition provides energy for microbial activity, while the C:N ratio affects the decomposition of organic matter by soil microorganisms (Gholz et al., 2010). The correlation results (Fig. 8) indicate that TOC had a weak positive correlation with  $\text{CO}_2$  emission ( $P > 0.05$ ), but the soil C:N ratio had a significant negative correlation with  $\text{CO}_2$  emission ( $P < 0.05$ ), indicating that nitrogen has a limiting effect on soil respiration by affecting microbial metabolism. Liu et al. (2019) have reported that N addition promotes  $\text{CO}_2$  emission from wetlands soil, and the effect of organic N input was significantly higher than that of inorganic N input. Organic carbon acts as a carbon source for the growth of plants and microorganisms, which boosts their respiration. Moreover, TOC has a significant correlation with  $\text{N}_2\text{O}$  emissions ( $P < 0.05$ ). Most heterotrophic microorganisms use soil organic matter as carbon and electron donors (Morley N and Baggs E M., 2010). Soil carbon sources have an important influence on microbial activity. Nitrifying or denitrifying microorganisms need organic matter to act as the carbon source during the assimilation of  $\text{NH}_3$  or  $\text{NO}_3^-$ . High content of organic matter in the soil can promote the concentration of heterotrophic nitrifying bacteria, consume dissolved oxygen in the medium, and cause the soil to become more anaerobic, thereby slowing down autotrophic growth nitrifying bacteria. This reduces the nitrification rate, ultimately promoting  $\text{N}_2\text{O}$  release. Enwall et al. (2005) studied the effect of long-term fertilization on soil denitrification microbial action intensity. They found that the soil with long-term organic fertilizer application has a significant increase in organic matter content, and consequently, a significant increase in denitrification activity. Typically, low soil C:N ratios are favorable for the decomposition of microorganisms, the most

suitable range being between 10 and 12 (Pierzynski et al., 1994). As Table 4 shows, N<sub>2</sub>O emission was significantly related to the soil C:N ratios ( $P < 0.05$ ), which means that denitrifying bacteria could use their endogenous carbon source for denitrification when the external carbon source was insufficient. Moreover, incomplete denitrification leads to the accumulation of NO<sub>2</sub>-N, which is conducive to N<sub>2</sub>O release. Meanwhile, due to the weak competitive ability of Nos to electrons, a low soil C:N ratio inhibits the synthesis of Nos, which is also a reason for N<sub>2</sub>O release. In this study, all sites in transects T1–T4 exhibited similar soil C:N ratios in the optimum range (Table 1), which is favorable for microbial decomposition. However, the soil C:N ratios in transect T5 were higher than those in the other transects, especially in the dry lake bed. Therefore, transect T5 showed severe mineralization and a low microbial decomposition rate.

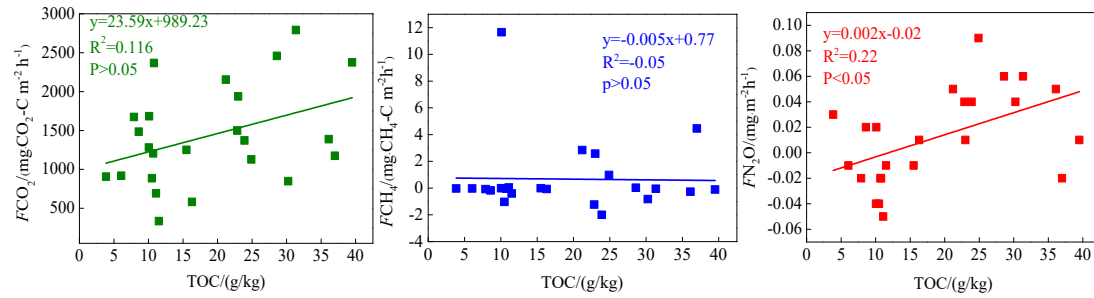


Fig. 8 Correlations between soil organic carbon (TOC) content and GHG emission ( $F$ )

Table 4. Correlations between CO<sub>2</sub>, CH<sub>4</sub>, and N<sub>2</sub>O emissions and impact factors ( $n = 62$ )

GHG flux	ST10	ST20	SMC10	SMC20	TOC	$\rho_b$	C:N	pH	EC	BIO
CO <sub>2</sub>	0.634**	0.592**	0.307*	0.216	0.393	-0.463**	-0.289*	-0.350**	-0.251*	0.491*
CH <sub>4</sub>	-0.029	-0.051	0.346**	0.353**	-0.02	-0.129	-0.156	-0.127	-0.107	0.607**
N <sub>2</sub> O	0.127	0.118	0.304*	0.356**	0.493*	-0.194	0.311*	0.137	0.504**	0.251

Note: 1. The analysis method used in the table is Pearson correlation analysis, and the numbers represent Pearson correlation coefficients.

2. \* and \*\* denote significant and highly significant correlations ( $P < 0.01$  and  $P < 0.05$ ), respectively.

3. ST - soil temperature, SMC - soil moisture content,  $\rho_b$  - soil bulk density, soil C:N - soil carbon-nitrogen ratio, pH - soil pH, EC - soil electrical conductivity, BIO - aboveground biomass

## 4.2 Riparian wetlands as hotspots of GHG emissions

The results of this study emphasized that the rate of CO<sub>2</sub> emission in the riparian wetlands were higher than that in the hillslope grasslands, owing to a variety of factors. ST is an important factor affecting GHG emission. Mclain and Martens (2006) showed that seasonal fluctuations in ST and SMC in semi-arid regions have important effects on CO<sub>2</sub>, CH<sub>4</sub>, and N<sub>2</sub>O emissions in riparian soils. Poblador et al. (2017) studied the GHG emission in forest riparian zones and suggested that the difference in the CO<sub>2</sub> and N<sub>2</sub>O emissions in these zones is caused by the spatial gradient of the regional SMC. In this study, the upstream riparian wetlands were characterized by higher TOC content, lower soil C:N ratio, and more abundant BIO than those in the hillslope grasslands (Table 1). These soil conditions benefited the soil microbial activity, ultimately enhancing respiration as well as CO<sub>2</sub> emissions. However, the CO<sub>2</sub> emission in the downstream areas was nearly identical to that in the grasslands, likely because the wetlands gradually evolved into grasslands after their degradation. N<sub>2</sub>O emission showed spatial patterns similar to that of CO<sub>2</sub> emission, likely because the CO<sub>2</sub> concentration was closely related to the nitrification and denitrification processes. High CO<sub>2</sub> concentrations can promote the carbon and nitrogen cycles in soil (Azam et al., 2005), increasing below ground C allocation, which is associated with increased root biomass, root turnover, and root exudation. Elevated pCO<sub>2</sub> in plants provides the energy for denitrification in the presence of high available N, and there is increased O<sub>2</sub> consumption under elevated pCO<sub>2</sub> (Baggs et al., 2003). Moreover, soil respiration increases during soil denitrification (Liu et al., 2010; Christensen et al., 1990). In this study, a weak correlation was observed between the CO<sub>2</sub> and CH<sub>4</sub> emissions in the riparian zones ( $r = 0.228$ ), but CO<sub>2</sub> emission was significantly correlated with N<sub>2</sub>O emission ( $r = 0.322$ ,  $P < 0.05$ ). The soil became anaerobic in the riparian areas as the SMC increased, and this was conducive to the survival of CH<sub>4</sub>-producing bacteria and to denitrification reactions, eventually leading to an increase in CH<sub>4</sub> and N<sub>2</sub>O emissions. Jacinthe et al. (2015) reported that inundated grassland-dominated riparian wetlands were CH<sub>4</sub> sinks ( $-1.08 \pm 0.22 \text{ kg} \cdot \text{CH}_4\text{-C ha}^{-1} \cdot \text{yr}^{-1}$ ), and Lu et al. (2015) also indicated that grasslands were CH<sub>4</sub> sinks. In our study, a marked water gradient across the transects led to the transformation of the soil from anaerobic to aerobic soil, which changed the wetland to either a CH<sub>4</sub> source or sink. Therefore, during the transition from the riparian wetlands to the hillslope grasslands, CH<sub>4</sub> sources only appeared in the near-stream sites, while sinks appeared at other sites.

Further, we compared the GHG emissions in the riparian wetlands and the hillslope

grasslands around the Xilin River Basin with those in various types of grasslands (meadow grassland, typical grassland, and desert grassland) in the Xinlingol League in Inner Mongolia (Table 5). CO<sub>2</sub> emission in the wet season decreased in the following order: upstream riparian wetlands > downstream riparian wetlands > hillslope grasslands > meadow grassland > typical grassland > desert grassland. Moreover, the upper riparian wetlands acted as sources of CH<sub>4</sub> emission, while the downstream transects and grasslands served as CH<sub>4</sub> sinks. Similarly, except in the downstream transects, N<sub>2</sub>O emissions occurred as weak sources in different types of grasslands and upstream riparian wetlands. The GHG emissions showed similar spatial patterns in October. Although these estimates were made only in the growing season in August and the non-growing season in October, our results suggest that the riparian wetlands are the potential hotspots of GHG emission. Thus, it is important to study GHG emission to obtain a comprehensive picture of the role of the riparian wetlands in climate change.

Table 5. GHG emission fluxes of riparian wetlands and grasslands

Sample plot	GHG emissions in August (mg·m <sup>-2</sup> ·h <sup>-1</sup> )			GHG emissions in October (mg·m <sup>-2</sup> ·h <sup>-1</sup> )			Reference
	CO <sub>2</sub>	CH <sub>4</sub>	N <sub>2</sub> O	CO <sub>2</sub>	CH <sub>4</sub>	N <sub>2</sub> O	
Wetlands of upstream transects (T1, T2, and T3)	n=13 1,606.28 ± 697.78	1.417 ± 3.41	0.031 ± 0.03	182.35 ± 88.26	0.272 ± 0.49	0.002 ± 0.005	This study
Wetlands of downstream transects (T4 and T5)	n=7 1,144.15 ± 666.50	-0.215 ± 0.45	-0.037 ± 0.05	98.13 ± 15.11	-0.015 ± 0.05	0.001 ± 0.01	
Hillslope grasslands of all transects	n=7 1,071.54 ± 225.39	-0.300 ± 0.40	0.003 ± 0.03	77.68 ± 25.32	-0.048 ± 0.03	-0.002 ± 0.005	
Meadow grassland	166.39 ± 45.89	-0.038 ± 0.009	0.002 ± 0.001	-	-	-	
Typical grassland	240.32 ± 87.56	-0.042 ± 0.025	0.037 ± 0.034	-	-	-	Guo et al., 2017
Desert grassland	107.59 ± 54.10	-0.036 ± 0.015	0.003 ± 0.001	-	-	-	Zhang, 2019
Typical grassland	520.25 ± 59.07	-0.102 ± 0.012	0.007 ± 0.001	88.34 ± 9.84	-0.099 ± 0.003	0.005 ± 0.001	
Typical grassland	232.42 ± 18.90	-0.090 ± 0.005	0.004 ± 0.001	-	-	-	Chao, 2019



Typical grassland	265.23 ± 31.43	-0.185 ± 0.018	0.005 ± 0.001	189.41 ± 28.96	-0.092 ± 0.012	0.004 ± 0.001
Meadow grassland	553.85	-0.163	0.003	47.73	-0.019	0.011
Typical grassland	308.60	-0.105	0.002	70.25	-0.029	0.007

Geng, 2004

We roughly estimated the annual cumulative emission amounts of CO<sub>2</sub>, CH<sub>4</sub>, and N<sub>2</sub>O from the riparian wetlands and hillslope grasslands around the Xilin River Basin, and further calculated their global warming potential. As Table 6 indicates, annual cumulative emissions of CO<sub>2</sub> and CH<sub>4</sub> decreased in the following order: upstream riparian wetlands > downstream riparian wetlands > hillslope grasslands, and N<sub>2</sub>O in the following order: upstream riparian wetlands > hillslope grasslands > downstream riparian wetlands. In this study, we used the static dark-box method to measure CO<sub>2</sub> emissions, which does not consider the absorption and fixation of CO<sub>2</sub> by plant photosynthesis. Therefore, the total annual cumulative CO<sub>2</sub> emissions are high. This result clearly showed the more significant impact of CO<sub>2</sub> emission than that of CH<sub>4</sub> and N<sub>2</sub>O emissions on global warming. The GWP depends on the cumulative emissions of the GHGs. The GWPs, shown in Table 6, were in the following order: upstream riparian wetlands (13,474.91 kg/hm<sup>2</sup>) > downstream riparian wetlands (8,974.12 kg/hm<sup>2</sup>) > hillslope grasslands (8,351.24 kg/hm<sup>2</sup>). Therefore, both the riparian wetlands and the grasslands are the “sources” of GHGs on a 100-year time scale. The source strength of the wetlands is higher than that of the grasslands, further indicating that the riparian wetlands are hotspots of GHG emission.

Table 6 Cumulative annual emission flux and global warming potential of GHGs in riparian wetlands and grasslands

Sample plot	CO <sub>2</sub> /kg/hm <sup>2</sup>	CH <sub>4</sub> /kg/hm <sup>2</sup>	N <sub>2</sub> O/kg/hm <sup>2</sup>	GWP/CO <sub>2</sub> kg hm <sup>2</sup>
Wetlands of upstream transects (T1, T2, and T3)	13,092.8±5378.16	12.36±26.40	0.25±0.23	13,474.91±5828.68
Wetlands of downstream transects (T4 and T5)	9,093.47±4831.82	-1.68±3.23	-0.26±0.40	8,974.12±4912.75
Hillslope grasslands of all transects	8,412.26±1614.26	-2.55±3.12	0.01±0.20	8,351.24±1648.22

### 4.3 Effects of riparian wetland degradation on GHG emissions

The hydrology and soil properties showed evident differences between transects because the downstream zone was dry all year due to the presence of the Xilinhote Dam (Fig. 1). The dam caused the degradation of the riparian wetlands, resulting in reduced GHG emission. The average CO<sub>2</sub> emission amounted to 1,663 mg·m<sup>-2</sup>·h<sup>-1</sup> in the upstream transects (T1, T2, and T3) at the riparian wetlands, while the downstream transects (T4 and T5) recorded an average emission of 1,084 mg·m<sup>-2</sup>·h<sup>-1</sup>, 35% lower than that in the upstream transects. The N<sub>2</sub>O emission from the riparian wetlands was lower in the downstream transects.

Wetland degradation first resulted in the continuous reduction of SMC, which led to the deepening of the wetland's aerobic layer thickness. Besides, SMC may affect ST and thus transport the CH<sub>4</sub> emissions from a source to a sink by affecting methanogen activity (Yan et al., 2018). Second, the reduction of SMC impeded physiological activities of aboveground plants and inhibited related enzyme activities in the respiration process. Meanwhile, various enzyme reactions of underground microorganisms under water stress influence and reduced CO<sub>2</sub> emissions (Zhang et al., 2017). Finally, after wetland degradation, long-term drought led to an extremely low SMC, which is not conducive to the growth of nitrifying and denitrifying bacteria and causes the transport of N<sub>2</sub>O emissions from source to sink (Zhu et al., 2013). As Table 1 shows, soil TOC content in the upstream transects (average: 25.1 g·kg<sup>-1</sup>) was higher than that in the downstream transects (average: 8.41 g·kg<sup>-1</sup>). The relatively low SMC and the aerobic environment were conducive to the mineralization and decomposition of the TOC. The degradation of plants in the wetlands led to the gradual reduction of BIO. Ultimately, the plant carbon source input of the degraded wetlands decreased, and the bare land temperature increased due to the reduced plant shelter. This accelerated the decomposition of TOC, leading to its decrease. This result indicates that wetland degradation caused the soil carbon pool's loss and weakened the wetland carbon source/sink function. These results are in agreement with those of Xia (2017).

The degraded wetlands also caused soil desertification and salinization, leading to a decline in the physical protection afforded by organic carbon and a reduction in soil aggregates. Thus, the preservative effect provided by organic carbon declined. The TOC content and SMC in the dry lake bed in transect T5 were relatively high; however, the GHG emission was very low along this transect because soil pH values increased after the degradation of the lake soil, exceeding the

optimum range required for microorganism activity. The soil C:N ratio was very high, resulting in severe mineralization and a low microbial decomposition rate, thus affecting the GHG emissions.

## **5. Conclusions**

The riparian wetlands in the Xilin River Basin constitute a dynamic ecosystem. The present spatial and temporal transfers in the studied biogeochemical processes were attributed to the changes in SMC, ST, and soil substrate availability. Our simultaneous analysis of CO<sub>2</sub>, CH<sub>4</sub>, and N<sub>2</sub>O emissions from the riparian wetlands and the hillslope grasslands in the Xilin River Basin revealed that the majority of the GHG emissions occurred in the form of CO<sub>2</sub>. Moreover, our results clearly illustrate a marked seasonality and spatial pattern of GHG emissions along the transects and in the longitudinal direction (i.e., upstream and downstream). SMC and ST were two critical factors controlling the GHG emissions. Moreover, the abundant BIO promoted the CO<sub>2</sub>, CH<sub>4</sub>, and N<sub>2</sub>O emissions.

The riparian wetlands are potential hotspots of GHG emissions in the Inner Mongolian region. However, the degradation of these wetlands has transformed the area from a source to a sink for CH<sub>4</sub> and N<sub>2</sub>O emissions and reduced CO<sub>2</sub> emissions, which has severely affected the wetland carbon cycle processes. Our results show that though the riparian wetlands have high CO<sub>2</sub> emissions, the wetlands are CO<sub>2</sub> sinks due to the photosynthesis of plants. Overall, our study suggests that anthropogenic activities have significantly changed the hydrological characteristics of the studied area, and that this can accelerate carbon loss from the riparian wetlands and further influence GHG emissions in the future.

## **Author Contributions**

Xinyu Liu, Xixi Lu and Ruihong Yu designed the research framework and wrote the manuscript. Xixi Lu and Ruihong Yu supervised the study. Xinyu Liu, Hao Xue, Zhen Qi, Zhengxu Cao and Zhuangzhuang Zhang carried out the field experiments and laboratory analyses. Z.Z. drew the GIS mapping in this paper. Tingxi Liu proofread the manuscript. Heyang Sun contributed much to the revised version of our manuscript.

## **Acknowledgements**

This study was funded by the National Key Research and Development Program of China (grant no. 2016YFC0500508), Major Science and Technology Projects of Inner Mongolia

Autonomous Region (grant nos. 2020ZD0009 and ZDZX2018054), National Natural Science Foundation of China (grant no. 51869014), Key Scientific and Technological Project of Inner Mongolia (grant no. 2019GG019), and Open Project Program of the Ministry of Education Key Laboratory of Ecology and Resources Use of the Mongolian Plateau (grant no. KF2020006).

### **Competing interests**

The authors declare no conflicts of interest.

### **References**

- Azam F., Gill S., Farooq S.: Availability of CO<sub>2</sub> as a factor affecting the rate of nitrification in soil, *Soil Biology & Biochemistry*, 37, 2141–2144, doi 10.1016/j.soilbio.2005.02.036, 2005.
- Baggs E.M., Richter M., Cadisch G., Hartwig U.A.: Denitrification in grass swards is increased under elevated atmospheric CO<sub>2</sub>, *Soil Biology and Biochemistry*, 35, 729–732, doi 10.1016/S0038-0717(03)00083-X, 2003.
- Beger M., Grantham H.S., Pressey R.L., Wilson K.A., Peterson E.L., Dorfman D., Lourival R., Brumbaugh D.R., Possingham H.P.: Conservation planning for connectivity across marine, freshwater, and terrestrial realms, *Biological Conservation*, 143, 565–575, doi 10.1016/j.biocon.2009.11.006, 2010.
- Brady N C.: *Nature and properties of soils*, New Jersey: Prentice-Hall, Inc., doi 10.2307/3894608, 1999.
- Cao M., Yu G., Liu J., Li K.: Multi-scale observation and cross-scale mechanistic modelling on terrestrial ecosystem carbon cycle, *Science in China Ser. D Earth Sciences*, 48, 17–32, doi 10.1360/05zd0002, 2005.
- Chao R.: *Effects of Simulated Climate Change on Greenhouse Gas Fluxes in Typical Steppe Ecosystem*, Inner Mongolia University, 2019.
- Cheng S and Huang J.: Enhanced soil moisture drying in transitional regions under a warming climate, *Journal of Geophysical Research-Atmospheres*, 121, 2542–2555, doi 10.1002/2015JD024559, 2016.
- Christensen S., Simkins S., Tiedje J M.: Temporal Patterns of Soil Denitrification: Their Stability and Causes, *Soil Science Society of America Journal*, 54, 1614, doi 10.2136/sssaj1990.03615995005400060017x, 1990.

642 Ding W., Cai Z., Tsuruta H.: Cultivation, nitrogen fertilization, and set-aside effects on methane  
643 uptake in a drained marsh soil in Northeast China, *Global Change Biology*, 10, 1801–1809, doi  
644 10.1111/j.1365-2486.2004.00843.x, 2010.

645 Enwall K., Philippot L., Hallin S.: Activity and composition of the denitrifying bacterial  
646 community respond differently to long-term fertilization, *Applied and Environmental*  
647 *Microbiology*, 71, 8335-8343, doi 10.1128/AEM.71.12.8335-8343.2005, 2005.

648 Fan X.: Research on nitrification potential and denitrification potential of soil in several farmland  
649 in China, Nanjing Institute of Soil Sciences, Chinese Academy of Sciences, 1995.

650 Ferrón S., Ortega T., Gómez-Parra A., Forja J.M.: Seasonal study of dissolved CH<sub>4</sub>, CO<sub>2</sub> and N<sub>2</sub>O  
651 in a shallow tidal system of the bay of Cádiz (SW Spain), *Journal of Marine Systems*, 66, 244–257,  
652 doi 10.1016/j.jmarsys.2006.03.021, 2007.

653 Geng H.: Study on Charactors of CO<sub>2</sub>, CH<sub>4</sub>, N<sub>2</sub>O Fluxes and the Relationship between Them and  
654 Environmental Factors in the Temperate Typical Grassland Ecosystem, Northwest Agriculture &  
655 Forestry University, 2004.

656 Gholz H.L., Wedin D.A., Smitherman S.M., Harmon M.E., Parton W.J.: Long-term dynamics of  
657 pine and hardwood litter in contrasting environments: toward a global model of decomposition,  
658 *Global Change Biology*, 6, 751–765, doi 10.1046/j.1365-2486.2000.00349.x, 2000.

659 Gou Q., Qu J., Wang G., Xiao J., Pang Y.: Progress of wetland researches in arid and  
660 semi-ariregions in China, *Arid Zone Research*, 1001–4675, 213–220, 2015.

661 Guo X., Zhou D., Li Y.: Net Greenhouse Gas Emission and Its Influencing Factors in Inner  
662 Mongolia Grassland, Chinese Grassland Society, 2017.

663 Heilman J.L., Cobos D.R., Heinsch F.A., Campbell C.S., McInnes K.J.: Tower-based conditional  
664 sampling for measuring ecosystem-scale carbon dioxide exchange in coastal wetlands, *Estuaries*,  
665 22, 584–591, doi 10.2307/1353046, 1999.

666 Inubushi K., Furukawa Y., Hadi A., Purnomo E., Tsuruta H.: Seasonal changes of CO<sub>2</sub>, CH<sub>4</sub> and  
667 N<sub>2</sub>O fluxes in relation to land-use change in tropical peatlands located in coastal area of South  
668 Kalimantan, *Chemosphere*, 52, 603–608, doi 10.1016/s0045-6535(03)00242-x, 2003.

669 IPCC.: Climate Change 2013: The Physical Science Basis. Contribution of Working, Working  
670 Group I of the IPCC, 43, 866–871, 2013.

671 Jacinthe P.A., Vidon P., Fisher K., Liu X., Baker M.E.: Soil Methane and Carbon Dioxide Fluxes

from Cropland and Riparian Buffers in Different Hydrogeomorphic Settings, *Journal of Environment Quality*, 44, 1080–1115, doi 10.2134/jeq2015.01.0014, 2015.

Johnson-Randall L.A., Foote A.L.: Effects of managed impoundments and herbivory on wetland plant production and stand structure, *Wetlands*, 25, 38–50, doi 10.1672/0277-5212(2005)025[0038:eomiah]2.0.co;2, 2005.

Koops J.G., Oenema O., Beusichem M.L.: Denitrification in the top and sub soil of grassland on peat soils, *Plant and Soil*, 184, 1–10, doi 10.1007/bf00029269, 1996.

Kou X.: Study on Soil Physicochemical Properties and Bacterial Community Characteristics of River Riparian Wetland in Inner Mongolia Grassland, Inner Mongolia University, 2018.

Liu C.: Effects of Nitrogen Addition on the CO<sub>2</sub> Emissions in the Reed (*Phragmites australis*) Wetland of the Yellow River Delta, China, Liaocheng University, 2019.

Liu C., Xie G., Huang H.: Shrinking and drying up of Baiyangdian Lake wetland: a natural or human cause? *Chinese Geographical Science*, 16, 314–319, 2006.

Liu F., Liu C., Wang S., Zhu Z.: Correlations among CO<sub>2</sub>, CH<sub>4</sub>, and N<sub>2</sub>O concentrations in soil profiles in central Guizhou Karst area, *Chinese Journal of Ecology*, 29, 717–723, doi 10.1016/S1872-5813(11)60001-7, 2010.

Liu J., Wang J., Li Z., Yu J., Zhang X., Wang C., Wang Y.: N<sub>2</sub>O Concentration and Its Emission Characteristics in Sanjiang Plain Wetland, *Chinese Journal of Environmental Science*, 24, 33–39, 2003.

Lu Y., Song C., Wang Y., Zhao Z.: Influence of plants on CO<sub>2</sub> and CH<sub>4</sub> emission in wetland ecosystem, *Acta Botanica Boreali-Occidentalia Sinica*, 27, 2306–2313, 2007.

Lu Z., Du R., Du P., Li Z., Liang Z., Wang Y., Qin S., Zhong L.: Effect of mowing on N<sub>2</sub>O and CH<sub>4</sub> fluxes emissions from the meadow-steppe grasslands of Inner Mongolia, *Frontiers of Earth Science*, 9, 473–486, doi 10.1007/s11707-014-0486-z, 2015.

Lv M., Sheng L., Zhang L.: A review on carbon fluxes for typical wetlands in different climates of China, *Wetland Science*, 11, 114–120, doi CNKI:SUN:KXSD.0.2013-01-020, 2013.

Malhl S.S., McGill W.B.: Nitrification in three Alberta soils: effects of temperature, moisture and substrates concentration, *Soil Biology and Biochemistry*, 14, 393–399, doi 10.1016/0038-0717(82)90011-6, 1982.

Mclain J E T., Martens D.A.: Moisture controls on trace gas fluxes in semiarid riparian soils, *Soil*

Science Society of America Journal, 70, 367, doi 10.2136/sssaj2005.0105, 2006.

Meng W., Wu D., Wang Z.: Control factors and critical conditions between carbon sinking and sourcing of wetland ecosystem, Ecology and Environmental Sciences, 20, 1359–1366, doi 10.1016/S1671-2927(11)60313-1, 2011.

Mitsch W.J., Gosselink J.G.: Wetlands (Fourth Edition), John Wiley & Sons Inc.: Hoboken, New Jersey, USA, 2007.

Mitsch W.J., Gosselink J.G., Anderson C.J., Anderson, C. J.: Wetland ecosystems: John Wiley & Sons, 2009.

Moldrup P., Olesen T., Schjønning P., Yamaguchi T., Rolston D.E.: Predicting the gas diffusion coefficient in undisturbed soil from soil water characteristics, Soil Science Society of America Journal, 64, 1588–1594, doi 10.2136/sssaj2000.64194x, 2000.

Morley N., Baggs E.M.: Carbon and oxygen controls on N<sub>2</sub>O and N<sub>2</sub> production during nitrate reduction, Soil Biology & Biochemistry, 42, 1864–1871, doi 10.1016/j.soilbio.2010.07.008, 2010.

Naiman R.J., Decamps H.: The ecology of interfaces: Riparian zones, Annual Review of Ecology & Systematics, 28, 621–658, doi 10.2307/2952507, 1997.

National Agricultural Technology Extension Service Center (NATESC): Technical specification for soil analysis, 2006.

Niu C., Wang S., Guo Y., Liu W., Zhang J.: Studies on variation characteristics of soil nitrogen forms, nitrous oxide emission and nitrogen storage of the *Phragmites australis*-dominated land/inland water ecotones in Baiyangdian wetland, Journal of Agricultural University of Hebei, 40, 72–79, 2017.

Pierzynski G M S., J.T., Vance, G.F.: Soils and Environmental Quality, 1994.

Poblador S., Lupon A., Sabaté S., Sabater F.: Soil water content drives spatiotemporal patterns of CO<sub>2</sub> and N<sub>2</sub>O emissions from a Mediterranean riparian forest soil, Biogeosciences Discussions, 14, 1–28, doi 10.5194/bg-14-4195-2017, 2017.

Qin S., Tang J., Pu J., Xu Y., Dong P., Jiao L., Guo J.: Fluxes and influencing factors of CO<sub>2</sub> and CH<sub>4</sub> in Hangzhou Xixi Wetland, China, Earth and Environment, 44, 513–519, 2016.

Sjögersten S., Wal R V.D., Woodin S.J.: Small-scale hydrological variation determines landscape CO<sub>2</sub> fluxes in the high Arctic, Biogeochemistry, 80, 205–216, doi 10.2307/20456398, 2006.

Sun Y., Wu H., Wang Y.: The influence factors on N<sub>2</sub>O emissions from nitrification and

denitrification reaction, *Ecology and Environmental Sciences*, 20, 384–388, doi 10.1631/jzus.B1000275, 2011.

Tong C., Wu J., Yong S., Yang J., Yong W.: A landscape-scale assessment of steppe degradation in the Xilin River Basin, Inner Mongolia, China, *Journal of Arid Environments*, 59, 133–149, doi 10.1016/j.jaridenv.2004.01.004, 2004.

Ulrike R., Jürgen A., Rolf R., Wolfgang M.: Nitrate removal from drained and reflooded fen soils affected by soil N transformation processes and plant uptake, *Soil Biology and Biochemistry*, 36, 77–90, doi 10.1016/j.soilbio.2003.08.021, 2004.

Waddington J.M., Roulet N.T.: Carbon balance of a boreal patterned peatland, *Global Change Biology*, 6, 87–97, doi 10.1046/j.1365-2486.2000.00283.x, 2000.

Whiting G.J., Chanton J.P.: Greenhouse carbon balance of wetlands: methane emission versus carbon sequestration, *Tellus B*, 53, 521–528, doi 10.3402/tellusb.v53i5.16628, 2001.

WMO.: WMO Statement on the State of the Global Climate in 2017, World Meteorological Organization, 2018.

Xi X., Zhu Z., Hao X.: Spatial variability of soil organic carbon in Xilin River Basin, *Research of Soil and Water Conservation*, 24, 97–104, 2017.

Xia P., Yu L., Kou Y., Deng H., Liu J.: Distribution characteristics of soil organic carbon and its relationship with enzyme activity in the Caohai wetland of the Guizhou Plateau, *Acta Scientiae Circumstantial*, 37, 1479–1485, doi 10.13671/j.hjkxxb.2016.0129, 2017.

Xu H., Cai Z., Yagi K.: Methane Production Potentials of Rice Paddy Soils and Its Affecting Factors, *Acta Pedologica Sinica*, 45, 98–104, doi 10.1163/156939308783122788, 2008.

Yan L., Zhang X., Wang J., Li Y., Wu H., Kang X.: Drainage effects on carbon flux and carbon storage in swamps, marshes, and peatlands, *Chin J Appl Environ Biol*, 24, 1023–1031, doi 10.19675/j.cnki.1006-687x.2017.11031, 2018.

Yu P., Zhang J., Lin C.: Progress of influence factors on N<sub>2</sub>O emission in farmland soil, *Environment and sustainable development*, 20–22, 2006.

Zhang D.: Effects of Different Grazing Intensities on Greenhouse Gases Flux in Typical Steppe of Inner Mongolia, Inner Mongolia University, 2019.



760 Zhang Y., Hao Y., Cui L., Li W., Zhang X., Zhang M., Li L., Yang S., Kang X.: Effects of extreme  
761 drought on CO<sub>2</sub> fluxes of Zoige alpine peatland, Journal of University of Chinese Academy of  
762 Sciences, 34, 462-470, 2017.

763 Zhang Z., Hua L., Yin X., Hua L., Gao J.: Nitrous oxide emission from agricultural soil land some  
764 influence factors, Journal of Capital Normal University: Natural Science Edition, 26, 114–120,  
765 2005.

766 Zhu X., Song C., Guo Y., Shi F., Wang L.: N<sub>2</sub>O emissions and its controlling factors from the  
767 peatlands in the Sanjiang Plain, China Environmental Sciences, 33, 2228–2234, 2013.

768 Zona D., Oechel W.C., Kochendorfer J., Paw U K.T., Salyuk A.N., Olivas P.C., Oberbauer S.F.,  
769 Lipson D.A.: Methane fluxes during the initiation of a large-scale water table manipulation  
770 experiment in the Alaskan Arctic tundra, Global Biogeochem Cycles, 23, doi  
771 10.1029/2009gb003487, 2009.